

Quantitative characterisation of acoustic emission source for composite failure mechanism under quasi-static three-point bending

Sze Kai LOW^{1,a*}, Benjamin Steven VIEN^{1,b}, Nik RAJIC^{2,c}, Cedric ROSALIE^{2,d},
Francis ROSE^{2,e}, Wing Kong CHIU^{1,f}

¹Department of Mechanical & Aerospace Engineering, Monash University, Clayton, VIC 3008, Australia

²Defence Science and Technology Group, 506 Lorimer Street, Fishermans Bend, VIC 3207, Australia

^aSzeKai.Low@monash.edu, ^bBen.Vien@monash.edu,
^cNik.Rajic@dst.defence.gov.au, ^dCedric.Rosalie1@dst.defence.gov.au,
^eFrancis.Rose@dst.defence.gov.au, ^fWing.Kong.Chiu@monash.edu

Keywords: Structural Health Monitoring, Three-Point Bending, Composite Structures, Acoustic Emission

Abstract. Fibre reinforced composites have been discovered to have superior material properties compared to traditional materials. However, composite structures do have weaknesses which is highly susceptible to damage from accidental impacts. Passive approaches have gained popularity in recent years as these can be implemented using less structurally and electrically obtrusive sensor installations. The fundamental hypothesis is that every distinct impact event has a unique modal signature that can be exploited to distinguish between damaging and nondamaging impacts, and to characterize the severity of damage. Preliminary research showed that the possibility to determine the progressive failure mechanism in composite specimens subjected to three-point bending. Each failure mechanisms have its corresponding frequency bandwidth, and it can be seen by plotting the spectrogram of time-frequency analysis. However, the limitation of time-frequency analysis for identifying failure modes arises from the fact that there can be a confluence of modes having more-or-less the same group velocity hence, having the same arrival time in a time-frequency plot for a given frequency. This overlap makes it problematic to identify modes unambiguously from a time-frequency analysis. The modes can be more clearly separated on the basis of dispersion curves obtained in the frequency-wavenumber space. This information paves way to the idea of developing a modal sensor that is capable of providing experimentally determined dispersion curves that can be expected to lead to a quantum advance in capability for modal identification, and hence for determining a far more accurate modal signature for various acoustic emission events.

Introduction

Fibre reinforced composites have many structural and functional advantages such as high mechanical resistance, lightweight and freedom of forms. In such, fibre composites are suitable as structural materials for high-value assets where a reduction in structural weight can enhance performance, reduced fuel consumption and improve energy efficiency of the overall system [1]. These high-value assets include but not limited to, civil and military aircraft [2], wind turbines which make a significant contribution towards renewable energy generation [3], and metal or plastic-lined composite pressure vessels that are used as fuel tanks for space vehicles and other applications [4,5]. However, composite structures do have weaknesses which is highly susceptible to damage from accidental impacts [1,6-10]. Multiple studies have been conducted and found that even relatively low-energy impacts that leave little to no visual evidence of damage can cause

substantial reductions of up to 60% in compressive strength [7,8], which presents an unacceptable risk of failure for such high-value or safety critical structures. An important development for the structural integrity management of such highvalue assets is the shift towards structural health monitoring (SHM) and condition-based maintenance [11-13], as opposed to the conventional approach of setting inspection intervals and scheduled maintenance, which can involve time-consuming disassembly procedures as well as costly downtime. SHM techniques can be classified into two main categories: active and passive monitoring. Active monitoring is where the structure is interrogated by built-in or surface-mounted actuators, the response is then monitored by sensors attached to the structure. On the other hand, passive monitoring is where the sensing system relies on naturally occurring events, such as impacts, for the actuation. Passive approaches have gained popularity in recent years as these can be implemented using less structurally and electrically less obtrusive sensor installations, which is an important consideration for industrial application. One of the desired goals is for passive SHM to relate to impact events to be able to distinguish between damaging and nondamaging impacts, and to further distinguish between structurally significant and insignificant levels of damage. A successful approach for addressing these objectives will provide clear benefits for improved structural integrity management of composite structures across a range of important industry sectors. Ultrasonic waves that are generated by impact events, which are referred to as acoustic emission (AE), propagate as guided waves in plate-like structures, with distinctive modes of propagation depending on the particular laminate lay-up and constituents. The fundamental hypothesis is that every distinct impact event has a unique modal signature, i.e., a unique set of amplitudes for each of the propagating modes, and that this modal signature can be exploited to distinguish between damaging and nondamaging impacts, and to characterize the severity of damage. During the lifespan of the composite laminates, it may be exposed to various form of loading which may cause different kinds of failure to happen, which includes matrix crack, delamination, and fibre fracture. For the failure of single or bundled brittle fibres, the crack speed is expected to be high, and the average length of crack propagation is expected to be relatively smaller. The maximum crack length is the fibre diameter for a single fibre filament failure. Based on the fundamentals mentioned above, this leads to the expectation of an increased bandwidth toward higher frequencies for this source type. For cracks growing between the fibres, such as within the matrix or along the interface between fibre and matrix the situation will be slightly different. Sound wave travels slower in polymer matrix materials, as such, the expected crack propagation speed is much slower compared to fibre failure. In addition, the average crack lengths are expected to be larger as the crack typically only comes to a rest if stopped by fibre filaments of different orientation or after long distances of propagation due to changes in the stress concentration in the region around the crack tip. Both effects lead to the conclusion that the typical bandwidth of such sources is less than compared to fibre failure. As the extension of such cracks may cover a range from micrometres to several millimetres in a realistic composite, this can be viewed as mostly a statistical effect. The application of acoustic emission on the failure analysis of composite laminates leads to a series of research outputs which mainly focused on three types of failure, namely, matrix crack, delamination, and fibre fracture. It was found that there is a frequency response range that corresponds to each failure mechanisms. For the frequency range of matrix crack, delamination, and fibre fracture, the frequency ranges are validated in the preliminary research, which is in accordance with the experiments performed in [14–18]. For example, Sause et al. [19] confirmed these frequency ranges through numerical study, which found that the frequency ranges for matrix crack, delamination, and fibre fracture are 100–300 kHz, 300–400 kHz, and 400–700 kHz respectively. Gutkin et al. [20] used competitive neural networks to analyse a carbon-fibre reinforced polymer composite and found that the frequency ranges for matrix crack, delamination, and fibre fracture are 0–150 kHz, 300–400 kHz, and 400–700 kHz. Huang et al. [15] used acoustic emission signal to analyse pure resin matrix with matrix crack,

resin matrix within a carbon fibre tow and pre-cuts delamination specimen and found that the frequency ranges are within 58–185 kHz, 190–290 kHz, and 405–455 kHz. To summarize, research showed that the frequency ranges of matrix crack, delamination, and fibre fracture are within 100–300 kHz, 400–550 kHz, and 600–750 kHz. Based on the above frequency ranges, failure mode identification can be performed. Any sorts of failure in the composite laminates will cause a drastic decrease in the strength and stiffness, which may eventually cause ultimate failure of equipment made from them. In order to improve the safety and reliability of such high-valued equipment, it is of importance to investigate the general progression of failure event in laminates and to characterize the acoustic wavefield that arises from the failure mechanism.

Materials and Methods

Three different composite lay-ups were self-manufactured in the Monash Mechanical Engineering Workshop using prepreg plies. The composite prepreg used to manufacture the composite specimen is made of high-strength carbon with a SE84LV epoxy as its matrix (HMC/Gurit SE84LV). The first specimen (specimen A) is a 0-degree laminate with a lamination code of $[0_4]_s$ which is designed to induce fibre break. The second laminate (specimen B) is a 90-degree laminate with a lamination code of $[0/90_8]$ designed to induce matrix crack and the third laminate (specimen C) which consists of 45-degree ply has a lamination code of $[+45/-45/0/90]_s$. The idea of manufacturing these three different laminates is to conduct a three-point bending test on the specimen to study the process of failure mechanism and to ultimately induce a specific failure mechanism on the composite specimen.

As shown in Figure 1, all of the laminate strips is 200 mm tall and 25 mm wide. The sides drawn in purple represents the placement of the supports, the red drawing in the centre represents the contact of the loading roller with the composite specimen. The mechanical loadings were performed at cross-head speed of 0.5 mm/min using a tensile machine (INSTRON 1185) with a load cell of 100kN (Fig. 2). Two AE sensors (PKWDI, from Physical Acoustics Corporation-MISTRAS Group), connected to a 26dB pre-amplification, were coupled with silicone grease on the same face of the sample. They are asymmetrically arranged from the center of the specimen with a distance of 50 mm for one and 60 mm for another. The acquisition threshold is determined when the specimen is situated on the three-point bend rig in contact with the loading roller at zero stress. For each specimen type, the acquisition threshold increased step by step in such a way to avoid the acquisition of any acoustic activity coming from the external environment including the vibration from the tensile machine or any background noise. Specimen A and C were loaded with a loading rate of 0.08mm/s whereas specimen B is loaded at 0.03mm/s.

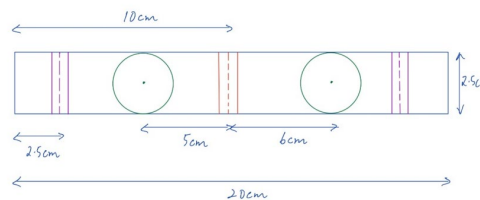


Figure 1: Schematic drawing of the laminate strip.

Composite laminates have complex failure modes, the main ones are known to be matrix crack, delamination, and fibre breakage. In order to investigate the evolution of failure in composite laminates, an experimental study was conducted on three laminates with different layups using acoustic emission technique. For the 0-degree laminate, a crack defect is imposed on the centre to induce fibre break. Three-point bend test are performed on the laminates and real-time acoustic emission signals are collected. Spectrograms can be constructed from the detected acoustic

emission signal and the evolution of failure mechanisms for different laminates with different ply lay-ups can be observed.



Figure 2: Experimentation setup for three-point bend test on composite specimens.

Results and Discussion

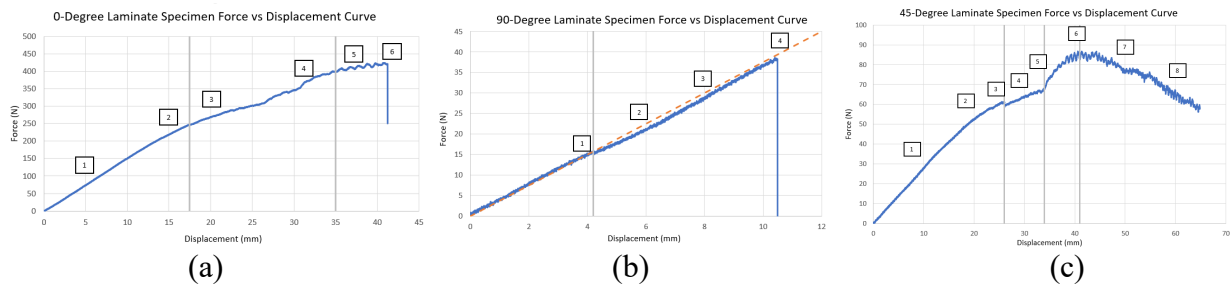


Figure 3: Force vs Displacement curve for (a) specimen A which has 6 points of investigation, (b) specimen B which has 4 points of investigation and (c) which has 8 points of investigation.

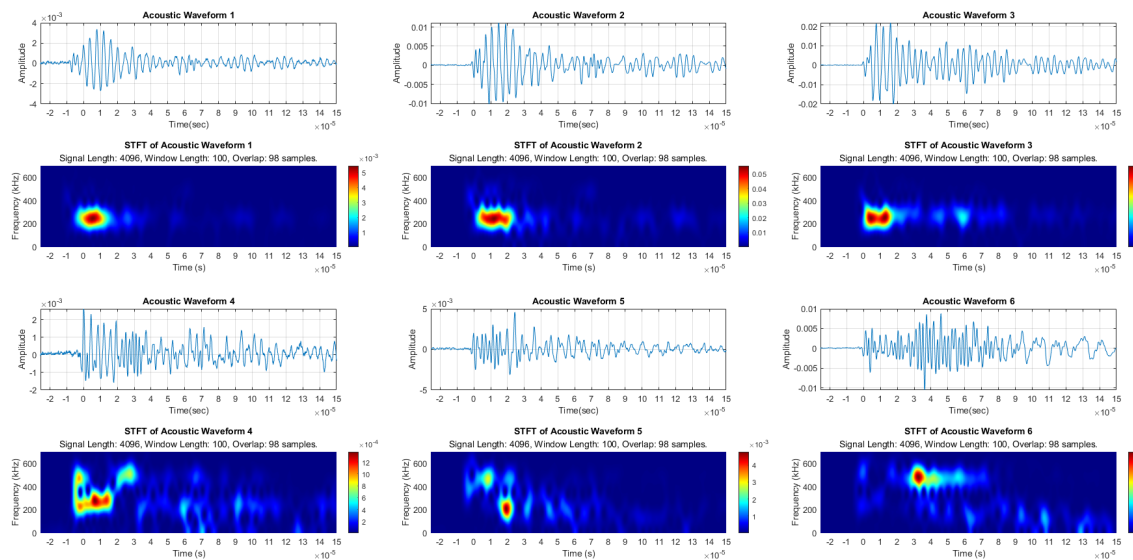


Figure 4: Analysis of time series and its corresponding spectrogram for specimen A.

To recall, bending of specimen A is to ultimately observe fibre fracture. Figure 3 (a) can be broken down into three significant regions. A total of 6 acoustic waveforms with 2 from each regions was used to analyse the failure mechanisms at those particular instances. The first region is between 0 mm to 17.5 mm displacement, where the force vs displacement curve is linear. In this region, two acoustic waveforms that were detected was used to analyse the failure mechanism that

has occurred in the specimen. Acoustic waveform 1 is the waveform detected at first hit which happens at the displacement of 5mm, whereas acoustic waveform 2 is the waveform detected at the displacement of 15mm, just before the second region. Analysis on the acoustic signal detected on this region showed that delamination caused by interlaminar shear is the dominant failure mode, and it happens at the start long before fibre breakage.

The second region is between the displacement of 17.5 mm to 35 mm, where the composite specimen starts to yield which is shown by the non-linearity of the force vs displacement curve. Acoustic waveform 3 is selected such that it is closer to the start of the second region and the waveform is detected at the displacement of 20 mm. Acoustic waveform 4 is selected towards the end of the region where a jump occurs on the force vs displacement curve at the displacement of 32mm. During this period of time, it is frequently observed that 3 failure mechanisms exist simultaneously, and the energy is higher compared to the previous region. The short-time Fourier transform of acoustic waveform 3 showed that at the start of the yielding process, the dominant failure mode is still delamination which is due to interlaminar shear. According to the short-time Fourier transform of acoustic waveform 4, it can be seen that not only lamina delamination occurs, but also fibre fracture which typically happens at the frequency range of 400kHz to 700kHz. This suggests that fibre fracture already starts to occur towards the end of the experiment but before the ultimate fracture point. At the end of the third region, ultimate failure occurs to the 0-degree composite laminate (specimen A) and the specimen breaks into half. Interestingly, from the start of the third region towards the end which leads to ultimate failure, the force and displacement curve exhibits oscillatory behaviour i.e., wave-like pattern. Acoustic waveform 5 was detected when the extension is at 37.5 mm, during where the force and displacement curve exhibits oscillatory behaviour. The last waveform investigated, which is acoustic waveform 6, is the last hit at the moment the composite specimen breaks into half. The short-time Fourier transform of acoustic waveform 5 showed that similar to acoustic waveform 4, fibre breakage and delamination both happens. At last, spectrogram of acoustic waveform 6 showed that the moment ultimate failure occurs, the only failure mode that exists is fibre fracture.

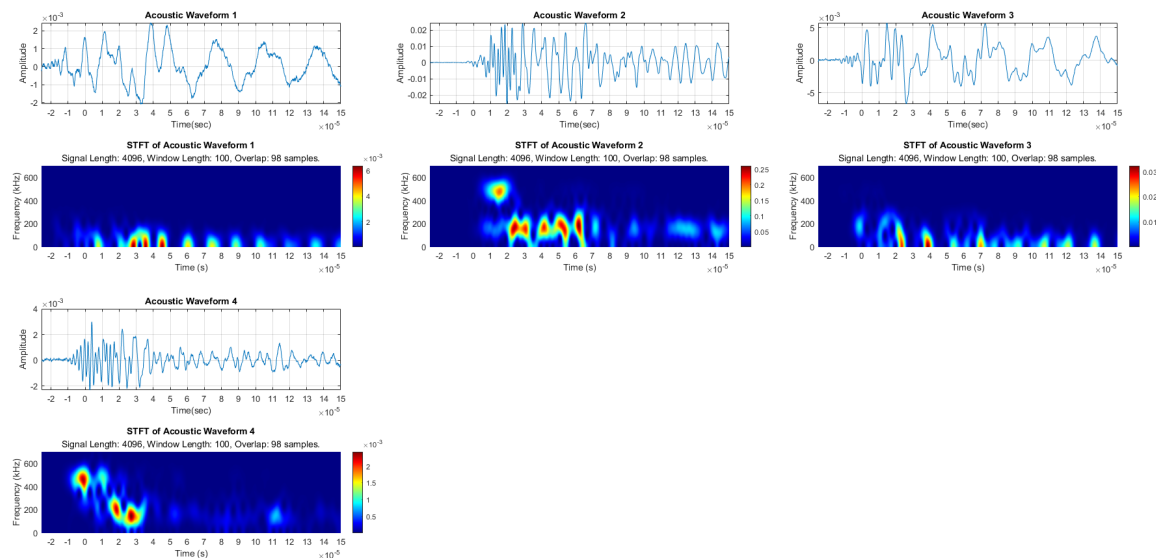


Figure 5: Analysis of time series and its corresponding spectrogram for specimen B.

Again, bending of the second laminate is to ultimately observe matrix crack. As shown in Figure 3(b), the force required to break the 90-degree laminate specimen (specimen B) is significantly lower compared to the 0-degree laminate specimen (specimen A) i.e., it is easier to induce matrix breaking compared to fibre fracture.

According to the AE software, hits were only starting to be registered at the displacement of 4.2 mm. That instance coincides with the sudden drop of force as shown on the figure above. Thus, the force vs displacement curve can be divided into two main regions. The first one is before the 4.2 mm displacement where none of the acoustic emission from the three failure modes were detected. Since no acoustic emission was detected, no waveform was analysed in this region. The second region starts at the displacement of 4.2 mm and ends at ultimate failure where the specimen breaks into half. Four acoustic waveforms were analysed to better investigate failure modes in this region. The corresponding waveforms were selected at the displacements of 4.2mm, 6mm, 8mm and 10.2mm. Acoustic Waveform 1 was detected when there is a sudden dip on the force vs displacement curve at the displacement of 4.2 mm. The short-time Fourier transform of acoustic waveform 1 showed that matrix cracking started happening at first hit detected. The short-time Fourier transform of acoustic waveform 2 showed that three failure mechanisms exist in the process of loading. Interestingly, fibre fracture failure can be detected which is suspected to be the breakage of fibres of the top layer 0-degree lamina. Spectrogram of acoustic waveform 3 showed that the three failure modes did not always happen simultaneously. Matrix crack is still the dominant failure mode at certain moments. All three failure modes can be detected at the end of the experiment where the composite specimen ultimately fails and breaks into half.

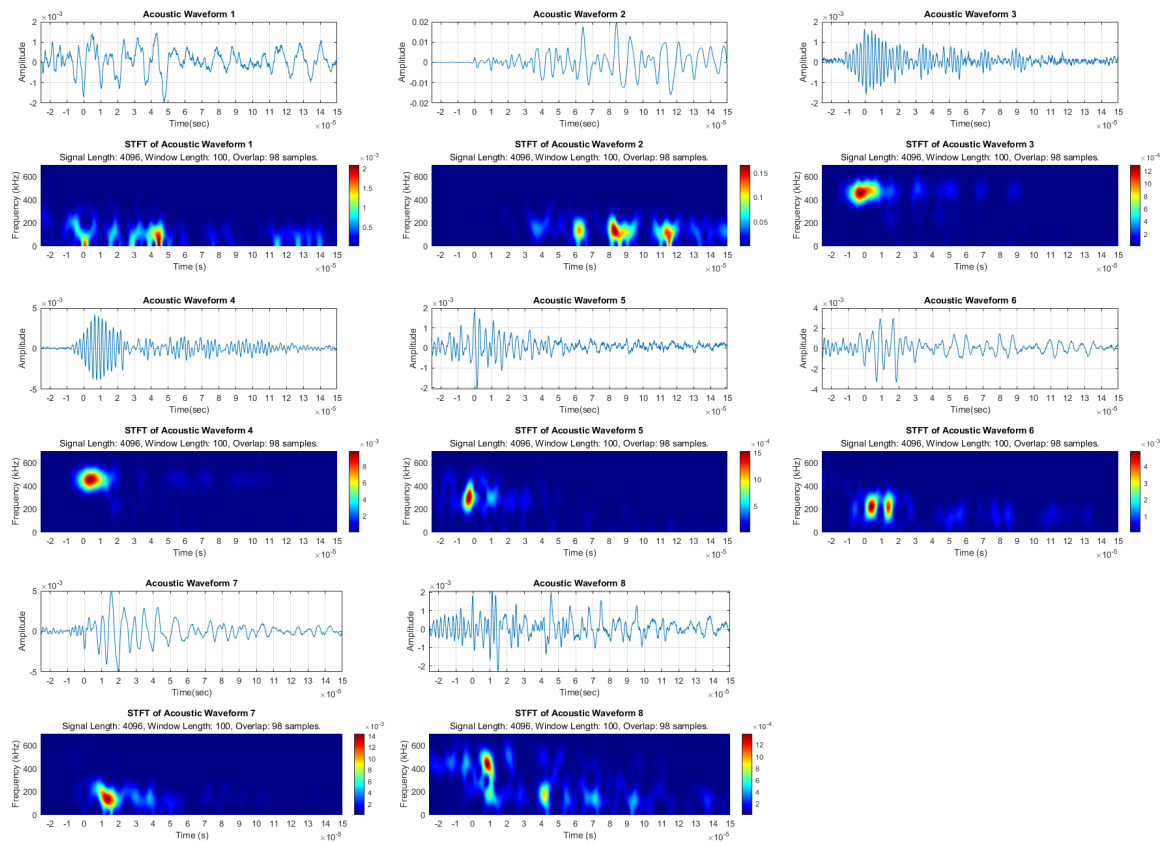


Figure 6: Analysis of time series and its corresponding spectrogram for specimen C.

Bending of the third laminate is to ultimately observe delamination. Figure 3(c) shown above can be divided into four main regions. The first region encompasses the start towards a displacement of 26 mm where the specimen is in the elastic region. The second region is selected at a displacement from 26.65 mm to 33.23 mm. There is a sudden dip on the force vs displacement curve at the start of this region followed by a linear increase of force against displacement. However, the slope is less steep compared to the first region. The third region is marked from a displacement of 33.23 mm towards the peak of the force vs displacement curve at 41.65 mm. It

can be observed that the force vs displacement curve is non-linear and the second half of the force vs displacement curve in this region exhibits oscillatory behaviour. The fourth region starts at the peak of the force vs displacement curve towards the end of the experiment. Interestingly, the force vs displacement curve decreases gradually in this region while also exhibit oscillatory behaviour. Note that for specimen C, no catastrophic failure or damage can be observed by the naked eye, and the experiment has to be put to an end manually.

Plenty of acoustic waveforms were detected during the experiment and the acoustic waveforms at multiple points of interests were selected for analysis to study the progressive failure mechanisms of the composite specimen throughout the experiment.

Acoustic waveform 1 and 2 is in the first region where the force vs displacement curve is linear. Acoustic waveform 1 is the first hit and it was detected at a displacement of 10 mm whereas acoustic waveform 2 was detected at a displacement of 20 mm. Acoustic waveform 3 is chosen because it was detected during the sudden dip of the force vs displacement curve. Acoustic waveform 4 is situated in the middle of the second region. Acoustic waveform 5 was detected when there is a rapid increase of the slope of the force vs displacement curve which ultimately leads to the peak of the force vs displacement curve where acoustic waveform 6 was detected. Acoustic waveform 7 and 8 was detected during the decrease of the force vs displacement curve at the displacements of 30 mm and 40 mm respectively.

Spectrogram of acoustic waveform 1 which is the first hit detected, showed that matrix crack is the first failure mode to occur at the beginning of the experiment. Acoustic waveform 2 showed that as time progresses, ply delamination starts to occur together with matrix cracking. Interestingly, spectrogram analysis on acoustic waveform 3 showed that fibre fracture occurs in the composite specimen, which could possibly explain the sudden drop of the force vs displacement curve at that moment. Acoustic waveform 4 showed that fibre fracture continues to happen in the second region as the force increases linearly against displacement. Acoustic waveform 5 was detected when there is a rapid increase of the slope of the force vs displacement curve. The spectrogram of the waveform showed that laminate ply delamination caused by interlaminar shear happens during that time period. At around the peak of the force vs displacement curve, interlaminar shear has been found to be the dominant failure mode. Spectrogram of the acoustic waveform 7 and 8 showed that during the time period where the force vs displacement curve is headed downwards, all three failure mechanisms can be detected.

Summary

In conclusion, this experiment studied the progressive failure mechanism in composite specimens subjected to loading. Each failure mechanisms have its corresponding bandwidth, and it can be clearly seen using spectrogram analysis. As mentioned in the introduction, the fundamental hypothesis is that every distinct impact event has a unique modal signature, and this modal signature can be exploited to distinguish between damaging and nondamaging impacts, and to characterize the severity of damage. However, the limitation of time-frequency analysis for identifying failure modes arises from the fact that there can be a confluence of modes having more-or-less the same group velocity hence, having the same arrival time in a time-frequency plot for a given frequency. This overlap makes it problematic to identify modes unambiguously from a time-frequency analysis. The modes can be more clearly separated on the basis of dispersion curves obtained in the frequency-wavenumber space. Thus, a modal sensor that is capable of providing experimentally determined dispersion curves can be expected to lead to a quantum advance in capability for modal identification, and hence for determining a far more accurate modal signature for various acoustic emission events.

References

- [1] Baker, A. A. Scott, M. L. (2016), Composite materials for aircraft structures 3rd Edition, AIAA, (2016). <https://doi.org/10.2514/4.103261>
- [2] BOEING 787 From The Ground Up <https://www.boeing.com/>
- [3] Experiments with carbon fibre blades could make wind turbines more energy efficient <https://www.createdigital.org.au/>
- [4] Kezirian, M.T. (2018) AIAA <https://doi.org/10.2514/6.2011-7363>
<https://doi.org/10.2514/6.2011-7363>
- [5] Lugovtsova, Y., Bulling, J., Boller, C., Prager, J. (2019), Appl. Sci. 2019, 9, 4600; doi:10.3390/app9214600
- [6] Abrate, S. (1998) Impact on Composite Structures, CUP, Cambridge. <https://doi.org/10.1017/CBO9780511574504>
- [7] Davies, G.A.O. R. Olsson, (2004) Aeronautical Journal 108, pp 541-563. <https://doi.org/10.1017/S0001924000000385>
- [8] Shohag, M. A. S., E. C. Hammel, D. O. Olawale and O. I. Okoli (2017). Wind Engineering 41(3): 185-210. <https://doi.org/10.1177/0309524X17706862>
- [9] Prosser et al (2004) SHM for future aerospace vehicles <https://ntrs.nasa.gov/search.jsp?R=20040200975>
- [10] Prosser et al (2004) AE detection of impact damage on space shuttle <https://ntrs.nasa.gov/search.jsp?R=20040171467>
- [11] Airbus Technical Magazine, Flight Airworthiness Support Technology No. 54, Aug 2014.
- [12] Gardiner, G., (2015) SHM: NDT integrated aerostructures enter service, Composites World, July 2015.
- [13] Society of Automotive Engineers, Guidelines for Implementation of SHM on Fixed Wing Aircraft, standards.sae.org/arp6461, 2013.
- [14] P. F. Liu, J. K. Chu, Y. L. Liu, and J. Y. Zheng, “A study on the failure mechanisms of carbon fibre/epoxy composite laminates using acoustic emission,” Materials & Design, vol. 37, pp. 228–235, 2012. <https://doi.org/10.1016/j.matdes.2011.12.015>
- [15] C. Huang, S. Ju, M. He et al., “Identification of failure modes of composite thin-ply laminates containing circular hole under tension by acoustic emission signals,” Composite Structures, vol. 206, pp. 70–79, 2018. <https://doi.org/10.1016/j.compstruct.2018.08.019>
- [16] D. Baccar and D. Soffker, “Identification and classification of failure modes in laminated composites by using a multivariate statistical analysis of wavelet coefficients,” Mechanical Systems and Signal Processing, vol. 96, pp. 77–87, 2017. <https://doi.org/10.1016/j.ymssp.2017.03.047>
- [17] M. R. Venturini Autieri and J. M. Dulieu-Barton, “Initial studies for AE characterisation of damage in composite materials,” Advanced Materials Research, vol. 13-14, pp. 273–280, 2006. <https://doi.org/10.4028/www.scientific.net/AMR.13-14.273>
- [18] H. Jeong and Y.-S. Jang, “Wavelet analysis of plate wave propagation in composite laminates,” Composite Structures, vol. 49, no. 4, pp. 443–450, 2000. [https://doi.org/10.1016/S0263-8223\(00\)00079-9](https://doi.org/10.1016/S0263-8223(00)00079-9)
- [19] M. G. Sause, “Acoustic emission source identification in large scale fibre reinforced composites,” Journal of Acoustic Emission, vol. 33, p. S223, 2016.
- [20] R. Gutkin, C. J. Green, S. Vangrattanachai, S. T. Pinho, P. Robinson, and P. T. Curtis, “On acoustic emission for failure investigation in CFRP: pattern recognition and peak frequency analyses,” Mechanical Systems and Signal Processing, vol. 25, no. 4, pp. 1393–1407, 2011. <https://doi.org/10.1016/j.ymssp.2010.11.014>